

Cable Angle Feedback Control Systems to Improve Handling Qualities for Helicopters with Slung Loads

Christina M. Ivler*

Stanford University and US Army Aeroflightdynamics Directorate, Moffett Field, CA, 94035

Mark B. Tischler†

US Army Aeroflightdynamics Directorate, Moffett Field, CA, 94035

J. David Powell‡

Stanford University, Stanford, CA, 94305

The ability of a helicopter to carry externally slung loads makes the aircraft very versatile for many civil and military operations. However, the piloted handling qualities of the helicopter are degraded by the presence of the slung load. A control system is developed that uses measurements of the slung load motions as well as conventional fuselage feedback to improve the handling qualities for hover/low speed operations. Past research has been limited to studies focused on load damping, as opposed to the piloted handling qualities focus of this paper. The approach implements an explicit model following control system with cable angle feedback for the externally loaded UH-60 Black Hawk helicopter, which is optimized via multi-objective optimization software to simultaneously meet stability, performance, and handling qualities requirements. The improvements provided by this control system are demonstrated in a piloted fixed base UH-60 simulation. Pilot comments and statistics are presented to show the effectiveness of the cable angle feedback control system as compared to a baseline control system.

I. Nomenclature

LMR	Load Mass Ratio
UAV	Unmanned Aerial Vehicle
FCS	Flight Control System
RASCAL	Rotorcraft-Aircrew Systems Concepts Airborne Laboratory (Modified JUH-60 Black Hawk)
m_{load}	Mass of the externally slung load
$m_{aircraft}$	Mass of the aircraft without external load
Δ_{MAG}	Depth of magnitude notch in the aircraft attitude response near the load pendulum mode
ω_{-135}	Frequency where phase crosses through -135 degrees
\dot{x}	Derivative of states vector
x	States vector
u	Controls vector
A	Stability derivatives matrix
B	Control derivatives matrix
N	Coupling numerator

*PhD Candidate, Department of Aeronautics and Astronautics, Stanford University and Aerospace Engineer, U.S. Army Aviation and Missile Research, Development, and Engineering Center

† Senior Technologist and Flight Control Group Lead, U.S. Army Aviation and Missile Research, Development, and Engineering Center, AIAA Associate Fellow

‡ Professor Emeritus, Department of Aeronautics and Astronautics, Stanford University, AIAA Fellow

p, q, r	Aircraft roll, pitch, yaw rates in aircraft body axes with respect to inertial reference frame
u, v, w	Aircraft longitudinal, lateral, and vertical body axes velocities
ϕ, θ, ψ	Aircraft roll, pitch and yaw Euler angles with respect to inertial reference frame
$\delta_{lon}, \delta_{lat}$	Pilot control inputs for lateral and longitudinal cyclic
$\delta_{ped}, \delta_{col}$	Pilot control inputs for pedal and collective
ϕ_c, θ_c	Lateral and longitudinal cable Euler angles, with respect to the level heading reference frame
$\Delta\phi_c, \Delta\theta_c$	Relative lateral and longitudinal cable Euler angles, with respect to aircraft body frame
H	Compensator transfer function
k_p, k_ϕ, k_{ϕ_i}	Feedback gains for roll rate, roll attitude, and integral of roll attitude
k_C	Cable angle feedback
p_c, q_c	Roll and pitch cable angular rates, with respect to the inertial reference frame
$\delta_{a_{lat}}, \delta_{a_{lon}}$	Actuator commands for lateral and longitudinal control axes
$\delta_{a_{ped}}, \delta_{a_{col}}$	Actuator command for pedal and collective control axes
${}^N R^H$	Rotation matrix from the aircraft level heading coordinate system to the inertial coordinate system
${}^H R^C$	Rotation matrix from the cable coordinate system to the aircraft level heading coordinate system
${}^N R^L$	Rotation matrix from the load body coordinate system to the inertial coordinate system
${}^C R^L$	Rotation matrix from the load body coordinate system to the cable coordinate system
ϕ_l, θ_l, ψ_l	Lateral, longitudinal and heading Euler angles of the load, with respect the inertial reference frame.
σ_{tot}^2	Mean square value of the pilot input signal
σ_1^2	Half power of the pilot input signal, $\sigma_1^2 = \sigma_{tot}^2 / 2$
ω_1	Pilot cutoff frequency

II. Introduction

The operation of helicopters carrying externally slung loads has an important role in military and civilian applications for many diverse tasks such as delivering supplies, search and rescue, construction, fire-fighting, and logging. The additional utility of operating with a slung load comes at the cost of higher piloted workload due to the nature of controlling a two-body dynamic system: helicopter and slung load. The pilot must maneuver the helicopter effectively in order to fly to the drop-off point, as well as monitor load motions, and eventually place the load down in a precise location – often without visibility of the load from the cockpit. The indirect control of the slung load motions through the rotor is essentially a noncollocated control problem for the pilot, which are notoriously difficult.¹ It is well known that the presence of heavy external loads causes degraded piloted handling qualities ratings, especially for configurations with long slings and heavy loads.²

With the development of a prototype of the Heavy Lift Helicopter by Boeing in the 1970s came many ideas for automatically controlling helicopters with external loads. Some research focused on active controls placed *directly* on the external load, such as an active arm,³ or fins.⁴ The idea of using a feedback system to the rotor to *indirectly* damp the load motions by utilizing load cable angle feedback was investigated by Dukes,⁵ Gupta,⁶ Liu⁷ and Hutto.⁸ Lui and Gupta focused on optimal control methods for full-state feedback including load motions. Dukes and Hutto used classical control methods to improve load damping. Reference 7 provides a comprehensive trade-off study comparing these direct and indirect load controlling methods. It was found that the indirect feedback systems were more complex in implementation due to technological limitations at the time, but vastly more versatile in their effectiveness to differing load configurations as compared to devices installed directly on the external load. For the prototype Heavy Lift Helicopter, piloted evaluations were performed in flight to show that load damping could be improved with cable angle feedback, although pilot comments indicated that the system made the load feel heavier, which was not desirable.^{8,9}

Much of the modern research in the area of external load control for helicopters largely focuses on unmanned aerial vehicles (UAVs). The K-MAX helicopter UAV used cable angle feedback to aircraft controls (i.e. indirect control) to stabilize the load motions.¹⁰ Another example of indirect control is given in Ref. 11 which applied a feed forward technique previously used on overhead cranes to reduce swing motion on an unmanned autonomous Bergen

Industrial Twin (5.9 ft rotor diameter). Another study on small unmanned rotorcraft implemented delayed load state feedback to the rotor (indirect control) to damp load motions on the GT-Max (9.8 ft rotor diameter) and the indoor electric AAU Corona (2ft rotor diameter).¹²

Current literature on manned configurations has shown that conventional fuselage feedback control systems for helicopters with heavy external loads cannot provide adequate stability margins and simultaneously meet the military helicopter handling qualities specification (ADS-33E-PRF¹³) requirements, particularly in the roll axis.¹⁴ Reference 14 also analytically demonstrated for the CH-53K that adding an advanced feedback configuration including cable rate feedback can provide improved stability margins. Recent studies by the German Aerospace Center (DLR) largely focus on a flight director for the CH-53G helicopter, which does not use automatic control, but instead provides a display aid to the pilot for damping pendulous load motion.¹⁵ This method has proven very effective at damping unruly modes in forward flight. Recently, the DLR has also begun analytically exploring the use of rotor-state feedback for helicopter sling load positioning,¹⁶ and helicopter sling load damping.¹⁷

In previous research, where the main focus was to damp the load pendulum motions, the load feedback generally had the effect of making the load feel heavier to the pilot,⁹ and a heavier load is generally associated with poor maneuvering handling qualities.² This approach works well for a UAV, where handling qualities are not relevant, but may not be suitable for piloted operations. With the development of a flight validated external load handling qualities criteria in Ref. 2 to guide the control system design, this paper takes a different focus on improving handling qualities of the helicopter/slung load system.

This research focuses on the development of a full authority fly-by-wire flight control system (FCS) that implements cable angle feedback combined with conventional fuselage feedback to improve piloted handling qualities with an external load for hover/low speed operations. The fly-by-wire flight control system takes piloted control inputs and processes them through the flight control computer, which makes an appropriate command to the main and tail rotor actuators. Fly-by-wire provides a more flexible, full-authority architecture than legacy partial authority configurations used in previous manned literature on slung load control. The flight control system developed here does not require special or expensive equipment installed on the external load since a vision based or mechanical system (such as in the case of the K-MAX UAV¹⁰) can measure cable angles and rates from the fuselage.

The scope of this paper is to design an attitude command explicit model following flight control system using multi-objective optimization to meet hover/low speed ADS-33E-PRF¹³ specifications for a Level 1 helicopter as well as the slung load handling qualities and stability margin requirements. The control design with cable angle and rate feedbacks combined with standard fuselage feedbacks will be compared to a baseline control system that implements only traditional fuselage feedback. The results of a fixed based piloted simulation study are given to verify analytical results.

III. System Description

The aircraft considered in this paper is the RASCAL JUH-60 helicopter, which is operated by the Aeroflightdynamics Directorate of the US Army at Ames Research Center in Moffett Field, CA. The RASCAL, shown with an external load in Fig. 1, is a full authority, fly-by-wire system for the evaluation pilot, with a backup mechanical system for the safety pilot. It is used to research cockpit hardware, investigate rotorcraft handling qualities, and to develop and test new fly-by-wire control system architectures.¹⁸ This paper assumes a configuration of 15,000lb at low speed only, with a 5000 lb rectangular box external load, and 79 ft sling length. A useful measure of helicopter load is the load-mass-ratio (LMR), which is calculated by Eq. (1).

$$LMR = \frac{m_{load}}{m_{aircraft} + m_{load}} \quad (1)$$

Where the LMR for the configuration considered herein is 0.25. $LMR > 0.20$ are known to result in significant effects on handling qualities. This configuration, with high load-to-mass ratio and a long sling (79ft), was found to have particularly poor baseline handling qualities in Ref. 2, and therefore is good case for testing the benefits of cable angle feedback. However, the concept and conclusions developed here can be applied to any load configuration.



Figure 1. UH-60 with external load.

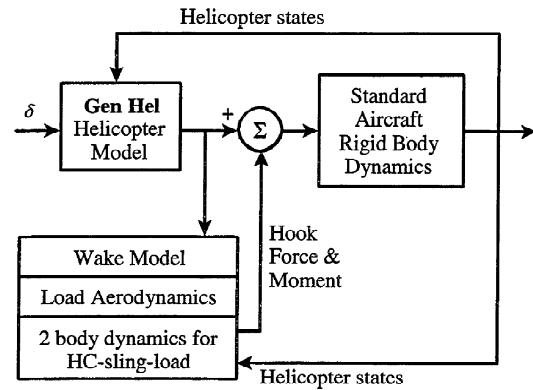


Figure 2: Slung load simulation diagram (Ref. 20).

The General Helicopter Flight Dynamics Simulation (GenHel) was used for nonlinear simulation of the unloaded UH-60 aircraft. GenHel is a full flight envelope, nonlinear, large angle model, with rigid blades and fuselage.¹⁹ It uses blade element theory for the main rotor and a Pitt-Peters Inflow model. The slung load dynamics are added via a module that simulates the load motion as a function of the helicopter states, and transmits hook forces and moments imparted by the external load up to the helicopter.²⁰ This process is depicted by Fig. 2. The model of helicopter and slung load is extensively validated against flight data in Ref. 20.

The linearized state-space model used for linear control design and analysis herein are derived from the nonlinear model via perturbation techniques. The tools used to extract these linear models are called FORECAST/OVERCAST and are described in Ref. 2. The linear model extracted for the hovering externally loaded UH-60 has 30 states: 9 fuselage, 4 slung load, 6 main rotor flap, 6 main rotor lag, 3 main rotor inflow, and 2 engine states. The resulting dynamic modes of the model are shown Table 1. The unstable pitch and roll Phugoid modes combined with the roll and pitch short period modes respectively, make up the unstable lateral and longitudinal hovering cubic behavior of a helicopter. The pendulum modes of the load (at ~ 1 rad/s) are stable, but lightly damped in the longitudinal case. An example validation of this linear model (with 56ft sling to match available flight data) against frequency responses identified from flight data using the CIPHER[®] fast Fourier transform (FFT) software²¹ is shown in Fig. 3. The figure indicates that the linear model provides a very good prediction of the flight responses.

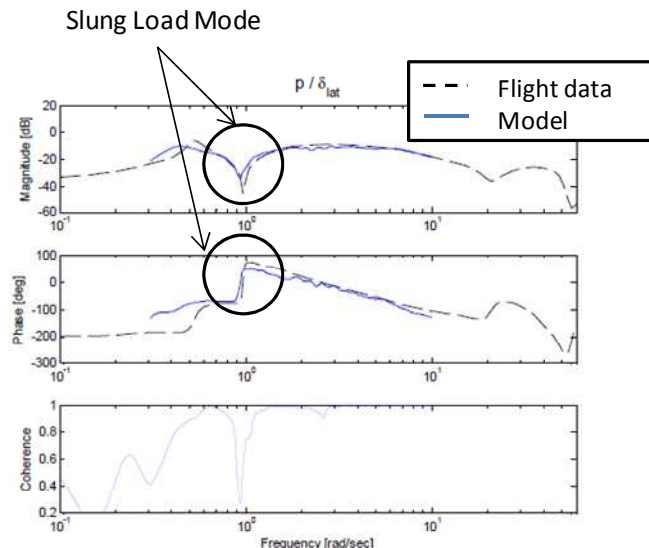


Figure 3. Model validation with 5K slung load, 56ft sling.

Table 1. Dynamic modes for 15,000lb UH-60 carrying a 5K lb external load on 79ft sling.

Mode Description	Eigenvalue	Frequency (rad/s)	Damping
psi integrator	-9.15E-16	0.00	1.00
Yaw/Heave	-2.45e-001 +/- 5.80e-002i	0.25	0.97
Pitch Phugoid	2.07e-001 +/- 3.97e-001i	0.45	-0.46
Roll Phugoid	3.79e-002 +/- 4.56e-001i	0.46	-0.08
Long. Pendulum	-1.24e-001 +/- 9.78e-001i	0.99	0.13
Pitch Short Period	-1.01	1.01	1.00
Lat. Pendulum	-7.31e-001 +/- 9.86e-001i	1.23	0.60
Collective Lead/Lag	-2.58e+000 +/- 1.01e+000i	2.77	0.93
Engine Response	-2.89	2.89	1.00
Roll Short Period	-4.87	4.87	1.00
Regressive Flap	-4.27e+000 +/- 4.76e+000i	6.39	0.67
Constant Inflow	-12.3	12.30	1.00
Regressive Lead/Lag	-5.77e+000 +/- 2.02e+001i	21.00	0.28
1st Harmonic Inflow	-2.04e+001 +/- 9.15e+000i	22.40	0.91
Collective Flap	-9.45e+000 +/- 2.56e+001i	27.30	0.35
Progressive Lead/Lag	-8.47e+000 +/- 3.61e+001i	37.10	0.23
Progressive Flap	-4.56e+000 +/- 4.86e+001i	48.90	0.09
Power Turbine Response	-90.8	90.80	1.00

IV. Slung Load Handling Qualities Specification

The recent development of a new slung load handling qualities criteria in Ref. 2 provides insight into how slung loads degrade handling qualities, and which aspects of the response the pilots find undesirable. This understanding shapes how the inclusion of the load feedbacks can be used to improve the pilot handling qualities of the load in this research. The slung load handling qualities specification is based on extensive flight test data where a variety of sling length and load masses were tested with the Mission Task Elements in ADS-33E-PRF.¹³ Mission Task Elements are a set of stylized maneuvers for helicopters which are performed by the pilot and rated based on the Cooper-Harper scale.

The slung load handling qualities specification that was developed relates the shape of the attitude frequency responses of the aircraft to the piloted handling qualities rating (HQR). An important characteristic of the response of an externally loaded helicopter is the depth of the notch in the attitude response (at 1 rad/s in Fig. 3) that is associated with the attenuation of the attitude response to pilot stick inputs because of the load swing. This notch is non-existent for an internally loaded baseline helicopter, and becomes deeper with increasing external load mass ratio (LMR) as shown in Fig. 4. The depth of the notch (Δ_{MAG}) as compared to an internally loaded helicopter is the metric used in y-axis of the handling qualities criterion shown in Figs. 5a-5b. As indicated by this criteria, a greater magnitude loss (caused by a heavier load) is associated with degrading handling qualities ($HQR > 4$). The x-axis criterion in Fig. 5 is the frequency of the -135 degree crossing of the phase response near the load mode (or the frequency of the minimum phase near the load mode if it does not cross -135 deg). The frequency where the phase crosses -135 degrees decreases with longer sling lengths, due to the lower frequency load pendulum mode (at approximately $\sqrt{(g/l)}$). This is associated with degraded handling qualities in Fig. 5. The -135 degree frequency is important because it is used in standard helicopter bandwidth criteria since it better correlates to helicopter handling qualities ratings than the pure magnitude bandwidth (-3dB frequency) that is often used in text books.²² Figure 5 also shows that the unaugmented configuration considered herein, with $LMR = 0.25$ and a 79ft sling, has poor handling qualities ($HQR > 4$).

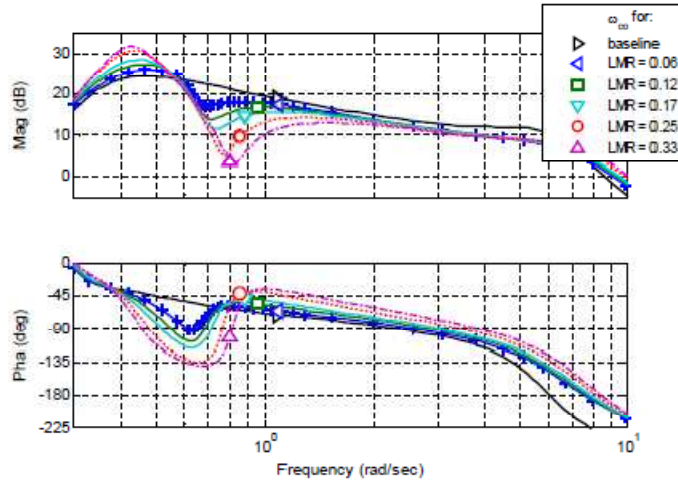


Figure 4. Roll attitude frequency response due to lateral cyclic for the 79ft sling with increasing LMR (Ref. 2).

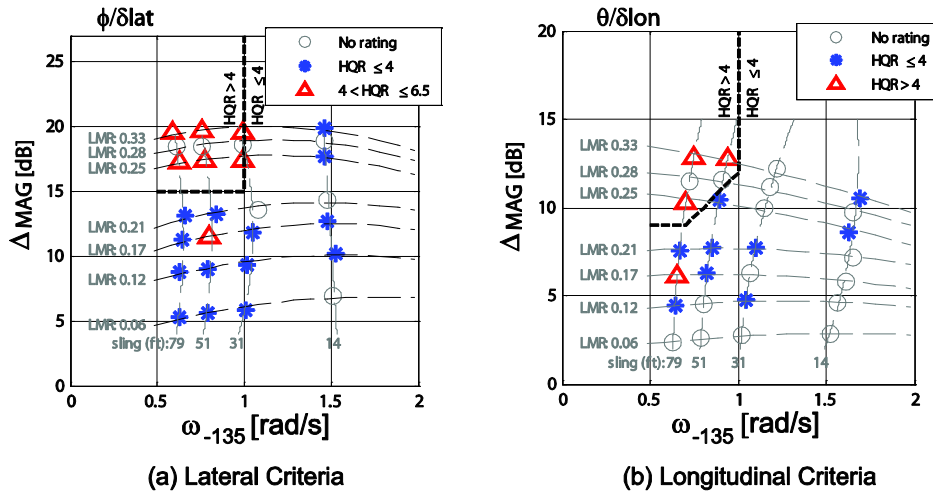


Figure 5. Slung load handling Qualities criteria (Ref. 2), where $HQR > 4$ represents poor handling.

Based on these criteria, the shape of the attitude response due to piloted stick determines how the slung load affects the piloted handling qualities. The data indicates that by reshaping the magnitude response via feedback control, the handling qualities of the externally loaded helicopter could be improved by manipulating the depth of the magnitude notch and the frequency of the -135 crossing. This approach would effectively cause the pilot to feel like he/she is flying a lighter load on a shorter sling.

V. Root Locus and Bode Designs: Simple Single Axis Examples

The key components of the control system were initially developed in a single axis environment in order to explore the first principles effects of cable angle feedback. In this approach, coupling numerators²³ are used to calculate the effective aircraft dynamics between a particular input and output pair, while the off-axis response variables are assumed to be tightly constrained by feedback. Then when designing control systems for the full order, fully coupled, multi-input multi-output system, where all the loops are simultaneously constrained by the control feedbacks, the analysis from the single-input coupling numerator is applicable.

A. Reduced Order Coupling Numerator Model

As an example of the calculation of coupling numerators, consider the following notional 4 degree-of-freedom system:

$$\dot{x} = Ax + Bu \quad (2)$$

$$A = \begin{bmatrix} a_{11} & a_{12} & a_{13} & a_{14} \\ a_{21} & a_{22} & a_{23} & a_{24} \\ a_{31} & a_{32} & a_{33} & a_{34} \\ a_{41} & a_{42} & a_{43} & a_{44} \end{bmatrix}, B = \begin{bmatrix} b_{11} & b_{12} & b_{13} \\ b_{21} & b_{22} & b_{23} \\ b_{31} & b_{32} & b_{33} \\ b_{41} & b_{42} & b_{43} \end{bmatrix} \quad (3)$$

$$x = [x_1 \quad x_2 \quad x_3 \quad x_4] \quad (4)$$

$$u = [\delta_1 \quad \delta_2 \quad \delta_3] \quad (5)$$

Then the single axis transfer function x_1/δ_1 , with x_2 tightly constrained by feedback of δ_2 , and x_3 tightly constrained by feedback of δ_3 , is given with the coupling numerator formulation following Ref. 23:

$$\frac{x_1}{\delta_1} \Big|_{\substack{x_2 \rightarrow \delta_2 \\ x_3 \rightarrow \delta_3}} = \frac{N_{\delta_1 \delta_2 \delta_3}^{x_1 x_2 x_3}}{N_{\delta_2 \delta_3}^{x_2 x_3}} = \frac{\begin{vmatrix} b_{11} & b_{12} & b_{13} & a_{14} \\ b_{21} & b_{22} & b_{23} & a_{24} \\ b_{31} & b_{32} & b_{33} & a_{34} \\ b_{41} & b_{42} & b_{43} & s - a_{44} \end{vmatrix}}{\begin{vmatrix} s - a_{11} & b_{12} & b_{13} & a_{14} \\ a_{21} & b_{22} & b_{23} & a_{24} \\ a_{31} & b_{32} & b_{33} & a_{34} \\ a_{41} & b_{42} & b_{43} & s - a_{44} \end{vmatrix}} \quad (6)$$

In a similar manner, the single-axis transfer functions are calculated for the lateral axis UH-60 with an external load. The lateral axis was chosen because it is more affected by the load motions than the longitudinal axis due to its lower inertial configuration. In this work we calculate the following lateral transfer functions:

$$\frac{p}{\delta_{lat}} \Big|_{\substack{q \rightarrow \delta_{lon} \\ r \rightarrow \delta_{ped} \\ w \rightarrow \delta_{col}}}, \frac{\phi}{\delta_{lat}} \Big|_{\substack{q \rightarrow \delta_{lon} \\ r \rightarrow \delta_{ped} \\ w \rightarrow \delta_{col}}}, \frac{\Delta \phi_c}{\delta_{lat}} \Big|_{\substack{q \rightarrow \delta_{lon} \\ r \rightarrow \delta_{ped} \\ w \rightarrow \delta_{col}}} \quad (7)$$

where the pitch rate is tightly constrained by longitudinal cyclic ($q \rightarrow \delta_{lon}$), the yaw rate is tightly constrained by the pedal ($r \rightarrow \delta_{ped}$), and vertical velocity is tightly closed by collective ($w \rightarrow \delta_{col}$). Comparisons of the bare airframe responses and the constrained (i.e. coupling numerator) responses for the roll attitude (ϕ) and load cable angle relative to the fuselage ($\Delta \phi_c$) are shown in Fig. 6. The responses are not strongly affected by the closure of the off-axis loops over the 1-10 rad/s range, but are more influenced in the 0.1-1 rad/s and 10-100 rad/s range where off-axis coupling is prevalent.

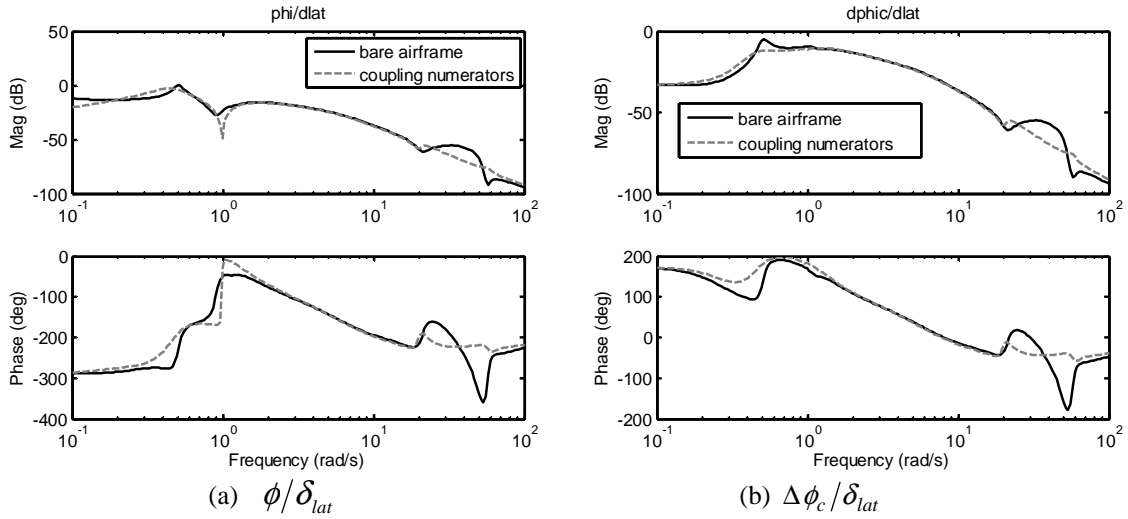


Figure 6. ϕ/δ_{lat} and $\Delta\phi_c/\delta_{lat}$ with and without coupling numerator closure of the off-axis dynamics.

Then, the order of the transfer function was reduced to simplify the calculations. This eliminated high frequency modes above 25 rad/s which did not have a large effect in the frequency range of interest for handling qualities, 0.1-10 rad/s.

B. Root Locus for Fuselage and Load Feedbacks

The use of the single axis coupling numerator transfer functions gives the root loci and bode plots for the lateral axis with the off-axes effectively closed. Three designs are examined:

- Fuselage Feedback Only
- Combination of Fuselage and Cable Angle Feedbacks
- Combination of Fuselage and Cable Rate Feedbacks

1. Fuselage Feedback Only

The effects of conventional fuselage feedback on the dynamic modes of the aircraft are seen in Fig. 7. As shown in Fig. 7a, roll rate feedback tends to initially improve the roll/flap-regressing mode and moves the Phugoid mode closer to the origin, but tends to reduce the damping of the lateral load pendulum mode. Roll attitude feedback in Fig. 7b tends to destabilize the roll/flap-regressing mode, but stabilizes the Phugoid mode and damps the load pendulum mode. Due to multiple constraints such as stability margin, disturbance rejection bandwidth, piloted bandwidth, etc., a combination of roll rate, roll angle, and the integral of roll angle feedbacks are required to provide a stable, and acceptably performing conventional control design for a helicopter.²⁴ As an example of a conventional feedback control system, a combination of feedbacks are used to form a PID compensator (H) for roll attitude in Fig. 7c via classical control techniques. The compensator architecture has the following form:

$$H = k_\phi \left[1 + \frac{k_p}{k_\phi} s + \frac{k_{\phi_i}}{k_\phi} \left(\frac{1}{s} \right) \right] \quad (8)$$

The following gains proportions were used to provide the ideal k/s loop shape in the region of cross-over (1-3 rad/s):

$$\frac{k_p}{k_\phi} = 0.8, \quad \frac{k_{\phi_i}}{k_\phi} = 0.2 \quad (9)$$

Then the root locus was calculated to determine the proper value of k_ϕ in Fig. 7c. The root locus indicates that increasing k_ϕ provides a better damped, higher frequency roll/flap-regressing mode (initially), as well as considerable improvement in Phugoid stability. However, increasing gain in Fig. 7c also results in a lightly damped, lower frequency load mode.

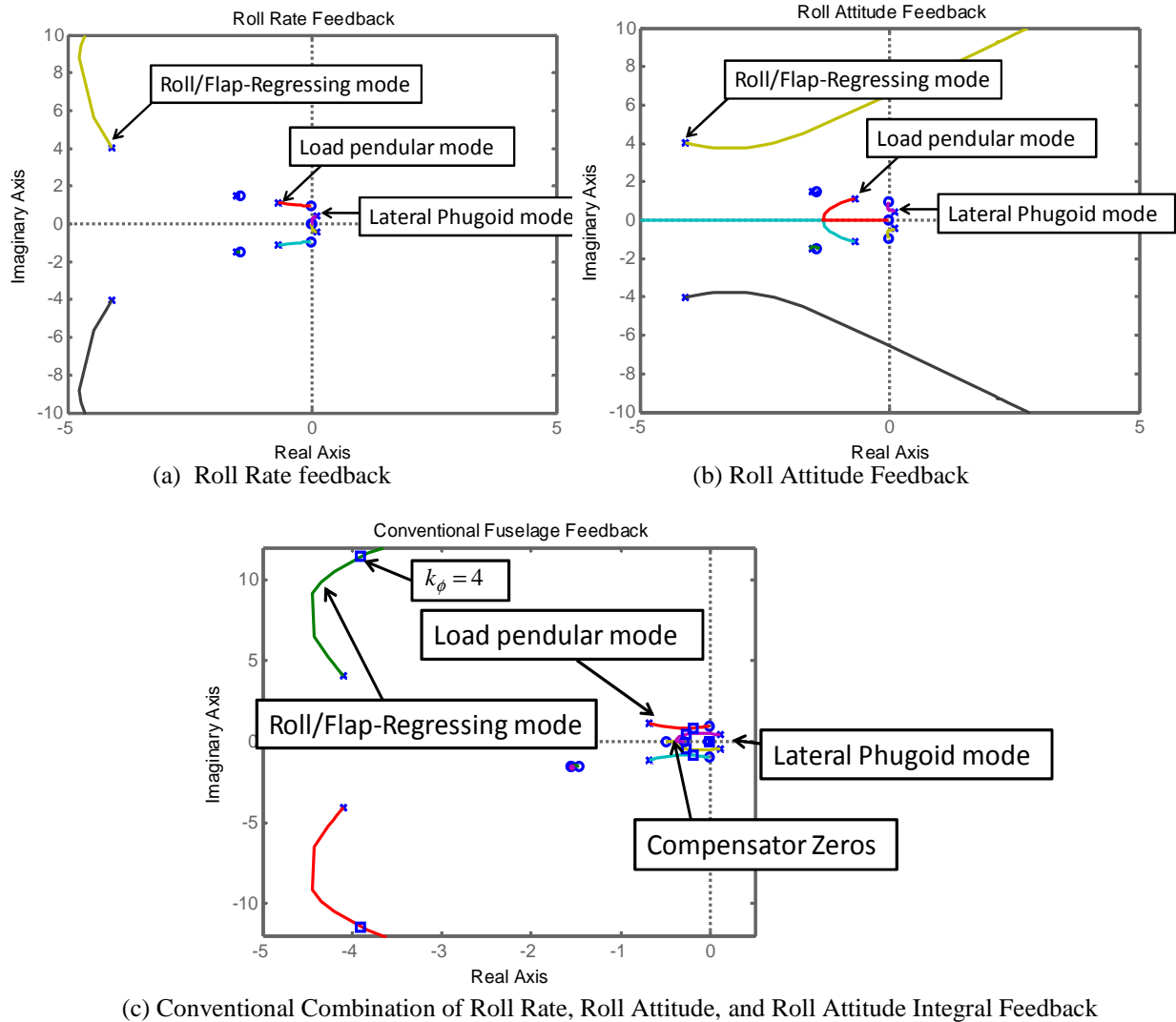


Figure 7. Root loci for fuselage feedback.

After choosing a gain of $k_\phi = 4$ for the conventional PID feedback from Fig. 7c, the closed loop bode plot of Fig. 8 indicates that the shape of the attitude response near the load mode are mostly unchanged as compared to the bare airframe. Although the closed loop gain has changed, and the steady state error has been eliminated, the depth of the magnitude notch of the slung load mode on the attitude is only slightly reduced, and the -135 deg frequency is unchanged. According to the slung load handling qualities specification, the maneuvering handling qualities with the external load have not greatly improved from the unaugmented case. The inertial referenced load motion (ϕ_c) is larger and not as well damped as the unaugmented system, as indicated by the magnitude peak at the load mode (~ 1 rad/s) in Figure 8b.

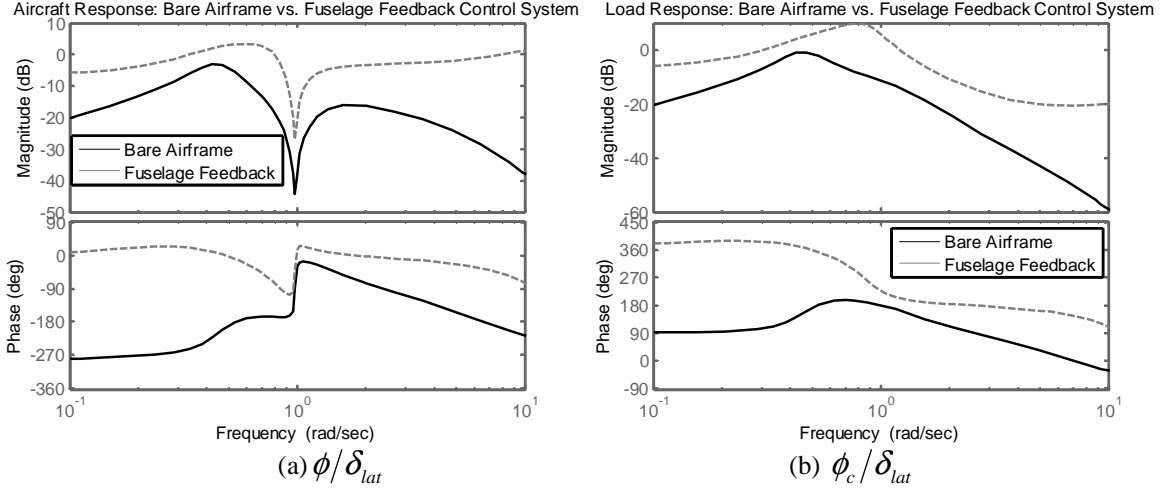


Figure 8: Bode plot comparison between bare airframe and fuselage feedback.

2. Fuselage and Cable Angle/Rate Feedback

The model provides states for the load cable parameters in a reference frame with respect to the fuselage. In this work, we have chosen to feedback the inertial referenced cable angle ϕ_c , as opposed to cable angle measured in a reference frame relative to the fuselage. In the single axis example, the fuselage referenced roll cable angle $\Delta\phi_c$ is simply:

$$\Delta\phi_c = \phi_c - \phi \quad (10)$$

In the single axis case, a combination of roll attitude feedback and inertial cable angle feedback can be algebraically manipulated to be equivalent to a compensator that uses roll attitude feedback combined with relative cable angle feedback via the relationship in Eq. (10). Although the two methods can be identically configured, the authors have chosen to use the inertial cable angle feedback in order to isolate the effect of the load swing on the control system. This also makes sense physically because the earth referenced (inertial) load swing response should be minimized in the hover/low speed configuration for precision load placement. Inertial cable rate feedback was also utilized in this analysis.

Choosing $k_\phi = 4$ from the root locus diagram in Figure 7c, and using the ratios for the rate and integral gains from Eq. (9), the characteristic equation adding inertial cable angle feedback k_C is:

$$1 + \frac{\phi}{\delta_{lat}} * 4 \left(1 + \frac{k_p}{k_\phi} s + \frac{k_{\phi_i}}{k_\phi} \left(\frac{1}{s} \right) + \frac{k_C \phi_c}{k_\phi \phi} \right) = 0 \quad (11)$$

Solving in Evans Root Locus Form for the cable angle feedback term, to isolate k_C , results in Eq. (12).

$$1 + \left(\frac{k_C \frac{\phi_c}{\delta_{lat}}}{1 + \frac{\phi}{\delta_{lat}} * 4 \left(1 + \frac{k_p}{k_\phi} s + \frac{k_{\phi_i}}{k_\phi} \left(\frac{1}{s} \right) \right)} \right) = 0 \quad (12)$$

In this root locus of Fig. 9, the poles represent the system with only the fuselage feedback control systems, $k_c = 0$. As cable angle feedback gain k_c increases, the closed loop poles change as shown in Fig. 9a, which does not improve load damping but further improves Phugoid mode damping from the baseline case. When using cable rate feedback instead of angular feedback in Fig. 9b, there is improved load damping, but a tendency for a lightly damped Phugoid mode.

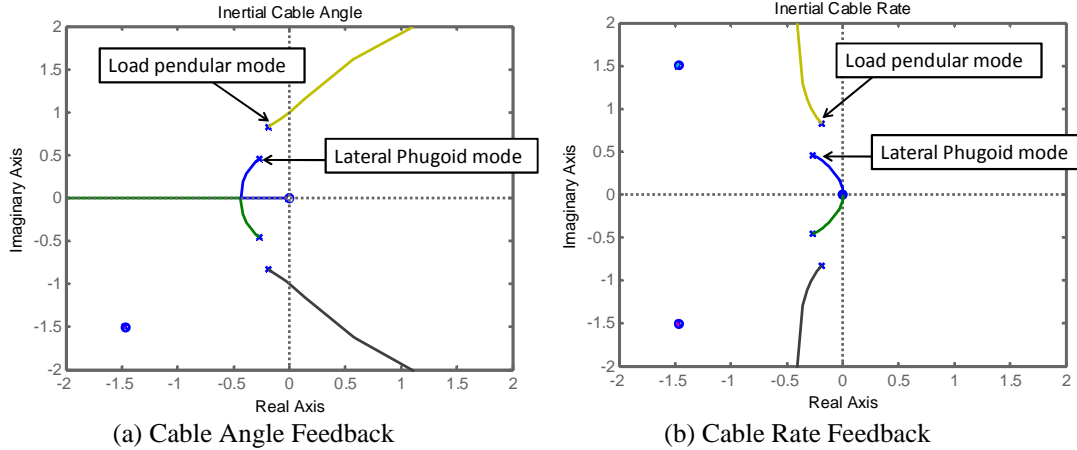


Figure 9. Root loci for cable angle feedback.

The result of cable angle and cable rate feedback on the closed loop response are shown in Fig. 10. Cable angle feedback in Fig. 10a provides a reduction (i.e. improvement) in the notch depth (smaller ΔMAG) as well as flattens the magnitude response between 0.2-0.9 rad/s. These effects combine to make a smoother attitude response which will provide better piloted handling qualities according to the slung load handling qualities specification. This feedback should effectively make the load feel “lighter” as it is increased. In Fig. 10b, the cable rate feedback creates a slightly deeper magnitude notch (larger ΔMAG), implying the load would feel effectively “heavier”, but will be better damped for load placement.

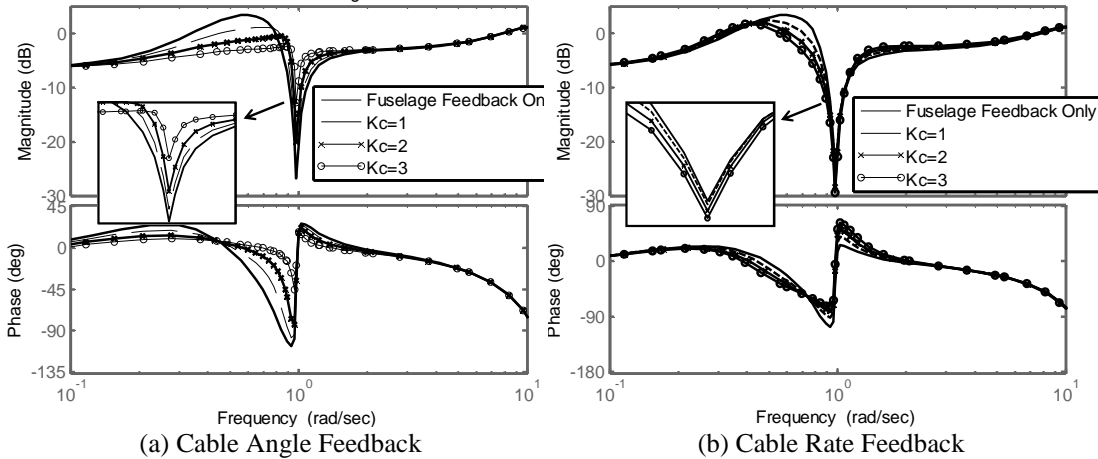


Figure 10. Aircraft response ϕ/δ_{lat} bode plot for combined fuselage and cable angle/rate feedback.

So, despite the benefits of better load handling qualities related to the cable angle feedback, the load becomes poorly damped, as indicated by Fig. 11a, which is consistent with the root locus shown in Fig. 9a. The load response damping is improved with cable rate feedback, as indicated by the phase response in Fig. 11b and the root locus of Fig. 9b. There is also a large attenuation of the cable angle magnitude between 0.5-1.1 rad/s with increasing cable rate feedback as shown by Fig. 11b. This indicates that the swing of the load will be much smaller with cable rate feedback.

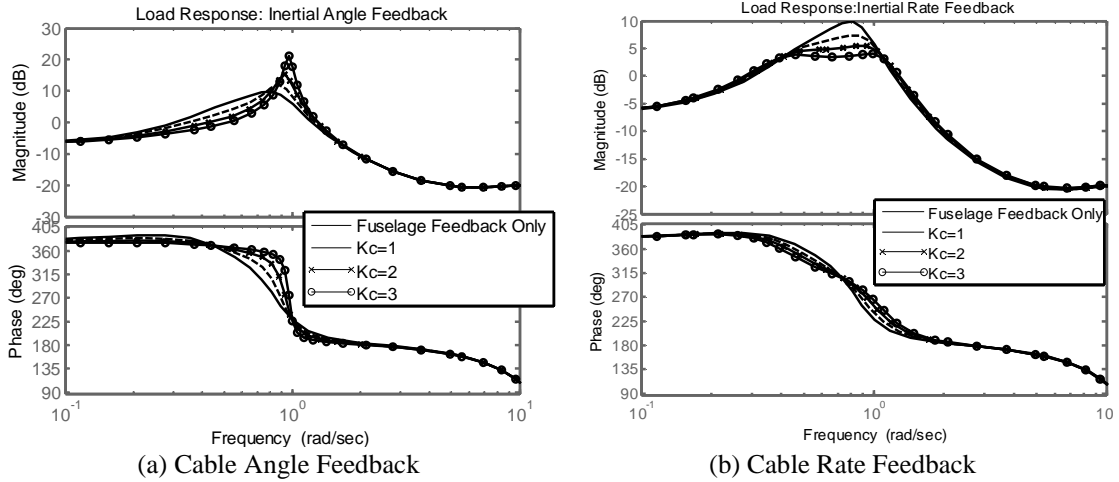


Figure 11. Load response ϕ_c / δ_{lat} bode plot for combined fuselage and cable angle/rate feedback.

These results indicate that cable angle feedback can be used to improve piloted handling qualities at the cost of a more lightly damped load response. The cable rate feedback does the opposite, providing a better damped load response, at the cost of degraded piloted handling qualities. This indicates that the right combination of cable angle and cable rate feedback could provide better handling qualities while maintaining the load damping at an acceptable level. The trade-off can be more fully explored via multi-objective optimization.

VI. Full Order Multi Objective Optimization with Cable Angle and Rate Feedback

The previous section explored the first principles dynamics and trade-offs of a helicopter/slung load flight control system. Now, the full order model presented in Sec. II is used for the design of an explicit model following control system with fuselage, cable angle and cable rate feedbacks. This control system architecture was chosen because it is an excellent approach for achieving handling qualities and feedback requirements for helicopters.²⁴ One key benefit of this architecture is that the bandwidth is set via the command model in the feed-forward path, independently of the feedbacks path, which sets disturbance rejection characteristics and stability margins. This is referred to as a 2 degree-of-freedom architecture class.²⁵ In contrast, for a simple feedback control system the bandwidth and disturbance characteristics are dependent upon one another, so increasing the disturbance rejection could result in an overly aggressive closed loop bandwidth.

The explicit model following architecture used in this work has the structure of Figs. 12-15, as implemented with slung load feedbacks in the lateral and longitudinal axes. There are no feedbacks of load states to the pedal and collective. Note that although each axis of the controller is shown independently in Figs. 12-15 for clarity, all controllers are simultaneously closed around the MIMO bare airframe state-space UH-60 model.

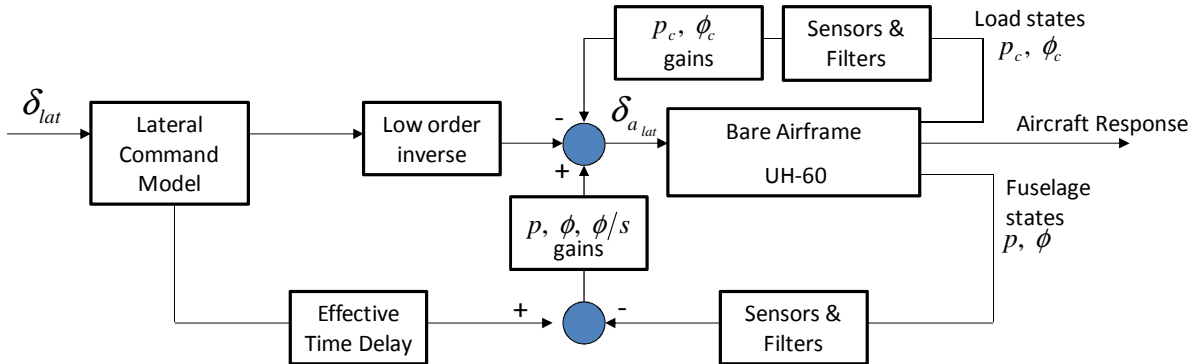


Figure 12. Lateral controller architecture.

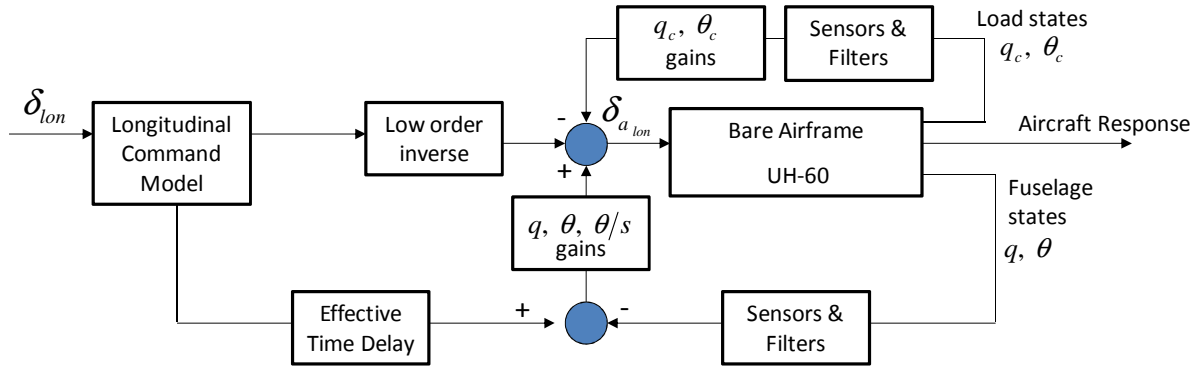


Figure 13. Longitudinal controller architecture.

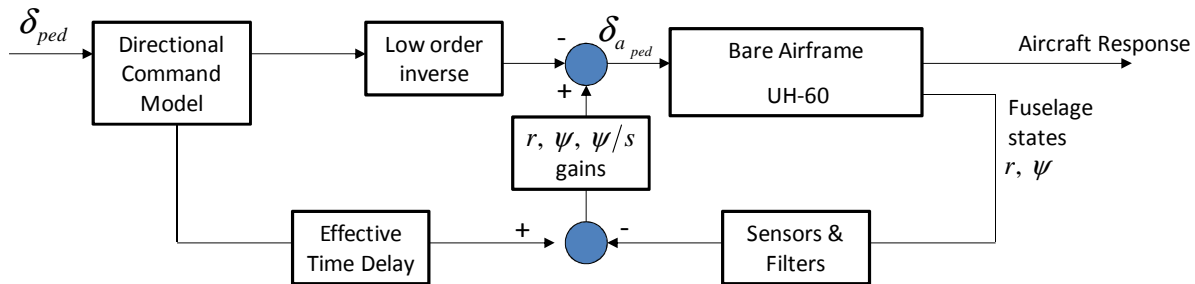


Figure 14. Yaw controller architecture.

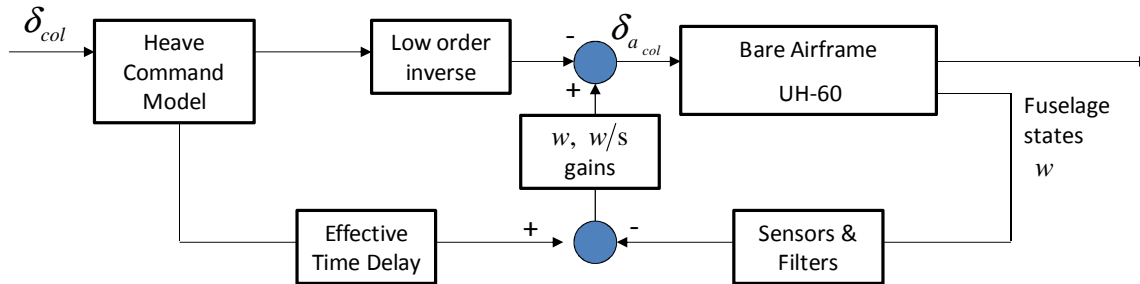


Figure 15. Heave controller architecture.

The structure of the model following controller and the purpose of each block are described in detail in Ref. 26. A short description of each block is provided below:

- Command Model - calculates the desired fuselage response for a given stick input.
 - Attitude command/ Attitude hold in the pitch and roll axes
 - Rate command/ Heading hold in the yaw axis
 - Vertical velocity command (with integrator for pseudo-altitude hold) in the heave axis
- Low Order Inverse - provides an estimate of the control input required to achieve the desired response.
- Effective time delay - accounts for the rotor and computational delays that are inherent in the aircraft, to avoid overdriving the feedback.
- Fuselage Feedback - compensates for errors in the inverse model, provides gust rejection and stabilizes the Phugoid mode.
- Load Feedback – provides load feedback to improve external load handling qualities.

A. Control Design Requirements

The control system was designed to meet the requirements for ADS-33E-PRF Level 1 handling, stability margins, disturbance rejection, and external load handling qualities. The design specifications of Table 2 were chosen to ensure that the control system would have the desired flying qualities. More background on these specifications is provided in Ref. 24.

Table 2. Control system design specifications.

Specification (CONDUIT Mnemonic)	Description	Constraint Type	Axes
EigLcG1	Eigenvalues in left-half plane	Hard	Pitch, Roll, Yaw, Heave
StbMgG1	Gain and Phase margin (45 deg, 6 dB)	Hard	Pitch, Roll, Yaw, Heave
BnwPiH1	Pitch bandwidth for acquisition and tracking, Attitude Command Requirements (ADS-33)	Soft	Pitch
BnwRoH2	Roll bandwidth for other M.T.E.'s, Attitude Command Requirements (ADS-33)	Soft	Roll
BnwYaH1	Yaw bandwidth for acquisition and tracking (ADS-33)	Soft	Yaw
BnwPiS1	Pitch External Load Handling Qualities Criteria (Lusardi, Ref. 2)	Soft	Pitch
BwnRoS1	Roll External Load Handling Qualities Criteria (Lusardi, Ref. 2)	Soft	Roll
CouPRH2	Coupling between pitch and roll	Soft	Pitch/Roll
CouYaH2	Coupling between collective and yaw	Soft	Yaw
DstBwG1	Disturbance rejection bandwidth	Soft	Pitch, Roll, Yaw, Heave
DstPkG1	Disturbance rejection peak magnitude	Soft	Pitch, Roll, Yaw, Heave
FrqHeH1	Heave response bandwidth (ADS-33)	Soft	Heave
HldNmH1	Normalized attitude hold response to disturbances	Soft	Pitch, Roll, Yaw
ModFoG2	Performance of Aircraft as compared to command model (model following)	Soft	Heave
OvsTimG1	Damping ratio	Soft	Pitch, Roll, Yaw, Heave
TrkErG1	RMS of load response in turbulence	Soft	Pitch, Roll
CrsLnG1	Minimizes Cross-over frequency	Summed Objective	Pitch, Roll, Yaw, Heave
RmsAcG1	Minimizes Actuator RMS	Summed Objective	Pitch, Roll, Yaw, Heave

There are many specifications that must be simultaneously achieved in order to provide a system with desirable flying qualities and a total of 13 feedback gains that must be chosen to meet these requirements. This is a difficult problem via classical control techniques which offer no direct way to assess and tune all these requirements simultaneously. Therefore, the control gains are determined with a multi-objective optimization technique.

B. Optimized Control Design

The CONDUIT[®] software is used to optimize the fuselage and load feedback gains. CONDUIT[®], the Control Designers United Interface, is a computational software package for aircraft flight control design, evaluation and

integration.²⁷ CONDUIT[®] is a useful tool because it combines the control system design process with the handling qualities requirements and servo-loop specifications compliance into one step. The control system is designed to meet these specifications with minimal control usage.

The design specifications are grouped into the three categories that define how the optimization prioritizes each requirement. The categories are known as Hard Constraints, Soft Constraints, and Summed Objectives. The specifications used for the optimization of the FCS in this research are grouped into these categories as indicated by the Constraint Type in Table 2. Hard constraints are considered in the first phase of the optimization. The set of Hard Constraints included requirements crucial to the stability of the aircraft (Eigenvalues in left-half plane and stability margins). During the second phase of the optimization soft constraints, which include handling qualities and performance criteria, must be satisfied while simultaneously ensuring that the Hard Constraints remain satisfied. The last phase of the optimization begins once all of the Hard and Soft Constraints are met. The optimization minimizes a set of Summed Objectives during this phase while ensuring that all other specifications continue to be met. Actuator RMS and crossover frequency are chosen as summed objectives to minimize control usage.

Three flight control systems were optimized to the required specifications in Table 2:

1. Baseline Control System – This control system is optimized to provide the best control system possible with conventional fuselage feedback only. This system does not use of cable angle feedback because it is meant to provide a baseline for comparison against the cable angle feedback control systems. By using the same architecture and optimizing against the same requirements, it provides the best possible comparison case for the two cable angle feedback designs.
2. Load Damping Control System – This control system attempts to meet the specifications while maximizing the external load damping. This control system uses fuselage, cable angle, and cable rate feedback.
3. Pilot Handling Control System– This control system provides the best piloted handling qualities possible by using the cable angle and rate feedback to smooth the attitude response, such that it better tracks the command model response and thus minimizes the effect of load swing on the helicopter’s attitude response.

A comparison of the key specifications is provided for the three optimized designs in Tables 3-4. The three designs are nearly identical in the yaw and heave axes, and so these axes are not shown in the tables for brevity. All margins and cross-over frequencies of Tables 3-4 are for open loop responses broken at the actuators in pilot axes. The model following cost described in these tables is a weighted, least-squared average of the magnitude and phase errors between the commanded and actual responses.²⁶ A lower model following cost indicates a better match between the commanded and actual responses.

Table 3. Key pitch axis metrics.

	Gain Margin	Phase Margin	Cross-over	Model Following	Δ MAG Load HQ spec	ω_{-135} Load HQ spec	Load Damping
	dB	deg	rad/s	Cost	dB	rad/s	nondim
Baseline	14.24	45.74	2.23	330.33	9.23	0.72	0.12
Load Damping	13.15	49.09	2.28	384.49	12.15	0.69	0.29
Pilot Handling	13.77	45.77	2.26	178.02	7.16	0.72	0.11

Table 4. Key roll axis metrics.

	Gain Margin	Phase Margin	Cross-over	Model Following	Δ MAG Load HQ spec	ω_{-135} Load HQ spec	Load Damping
	dB	deg	rad/s	Cost	dB	rad/s	nondim
Baseline	5.21	33.88	5.43	254.09	6.73	0.72	0.093
Load Damping	7.11	69.49	4.51	1233.58	13.77	0.46	0.27
Pilot Handling	6.08	45.39	4.75	168.58	5.42	0.69	0.13

The baseline control system cannot achieve more than 33 degrees of phase margin in the lateral axis, while the margin is improved above the desired 45 degrees when introducing cable angle feedback in both the load damping and pilot handling control systems. This indicates that slung load feedback can provide improved phase margins for the UH-60. The load feedback also improves the lateral gain margin, which is below the requirement of 6dB for the baseline case. The cross-over frequencies are not greatly affected by the slung load feedback.

As shown in the Tables 3-4, the pilot handling control system has the lowest model following cost in both the pitch and roll axes, indicating that it performs the most like the desired low order command model dynamics. The pilot handling control system has about the same load damping as the baseline case in the pitch axis, but exhibits improved load damping in the roll axis. The damping control system provides good load damping, but very poor model following. This is related to the sharp increase in the ΔMag of the attitude response for the load damping control system, indicating degraded handling qualities. Figure 16 shows that the slung load handling qualities for the baseline control system are acceptable in the roll axis, but are at the boundary for poor response in the pitch axis. The load damping case clearly exhibits worse aircraft handling qualities than either the baseline or the pilot handling control systems. The piloted handling case has improved handling qualities for roll and pitch axis, bringing the pitch axis well into the acceptable region. As indicated by Table 5, the pilot handling control system relies heavily on cable angle feedback, while the damping control system uses both cable angle and rate feedbacks.

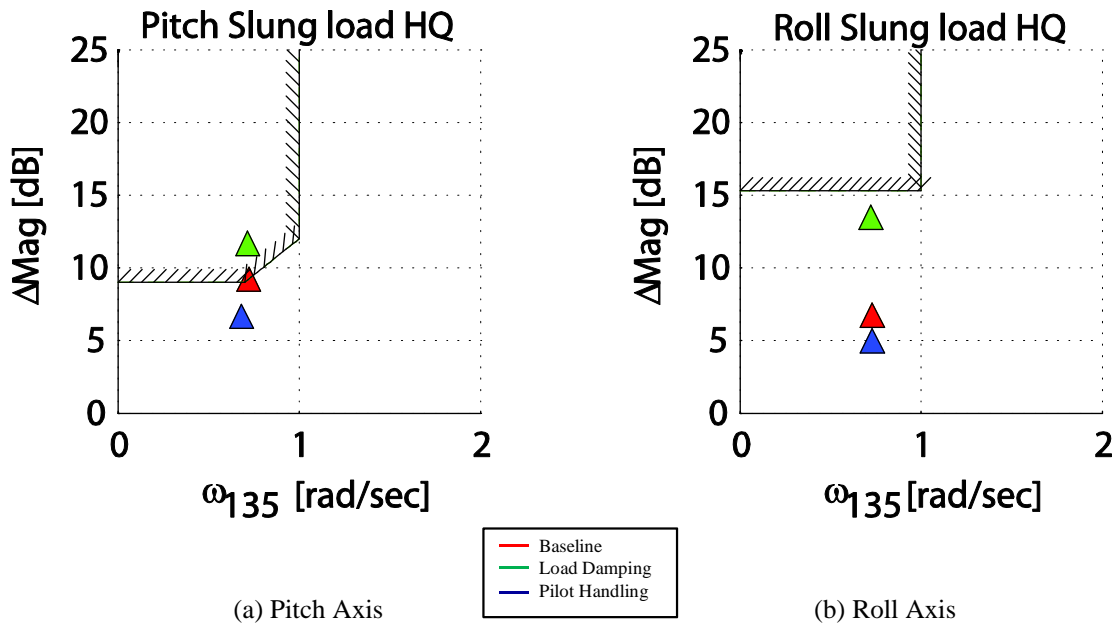


Figure 16. Slung load handling qualities specification for three optimized control systems.

Table 5. Load feedback parameters.

	Roll Axis Load Feedback Gains		Pitch Axis Load Feedback Gains	
	Cable Rate (in-s/rad)	Cable Angle (in/rad)	Cable Rate (in-s/rad)	Cable Angle (in/rad)
Baseline	0	0	0	0
Load Damping	7.89287	8.07536	1.4166	2.55865
Pilot Handling	0.0001	3.98154	0.0001	1.24166

Example closed loop frequency and time responses illustrate the trade-offs between the designs. Figure 17 overlays the closed loop roll attitude and lateral cable angle responses. As seen in the figure, the closed loop attitude

response is very smooth for the pilot handling control system, while the load damping has a large notch in the magnitude response. The load response is best for the load damping case and has the largest peak (worst damping) in the baseline design. The pilot handling case improves the peak load magnitude slightly as compared to the baseline. These results are consistent with the simple single axis results in Figs. 10-11, where the pilot handling control laws closely resemble the cable angle feedback cases and the load damping results are similar to the cable rate feedback.

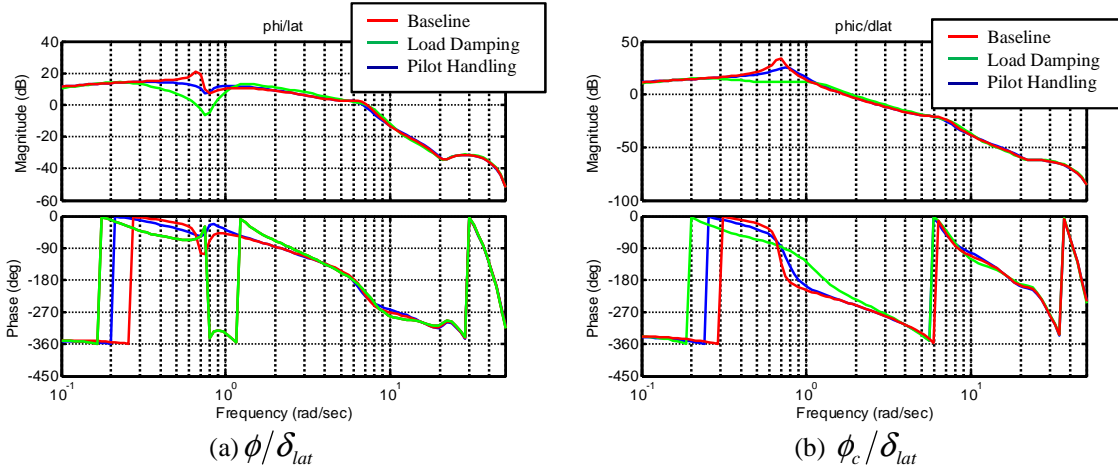


Figure 17. Closed loop bode plot overlays for three optimized control systems.

The time responses in Fig. 18 are consistent with the frequency responses of Fig. 17. As compared to the baseline control system, the pilot handling control system has a smoother fuselage response, with better damped residual aircraft attitude oscillations, as well as slightly better load damping. The load damping control system has a very poor fuselage response, with large uncommanded reversals in the attitude, but has excellent load damping. These results all show a clear tradeoff between load damping and maneuvering handling qualities.

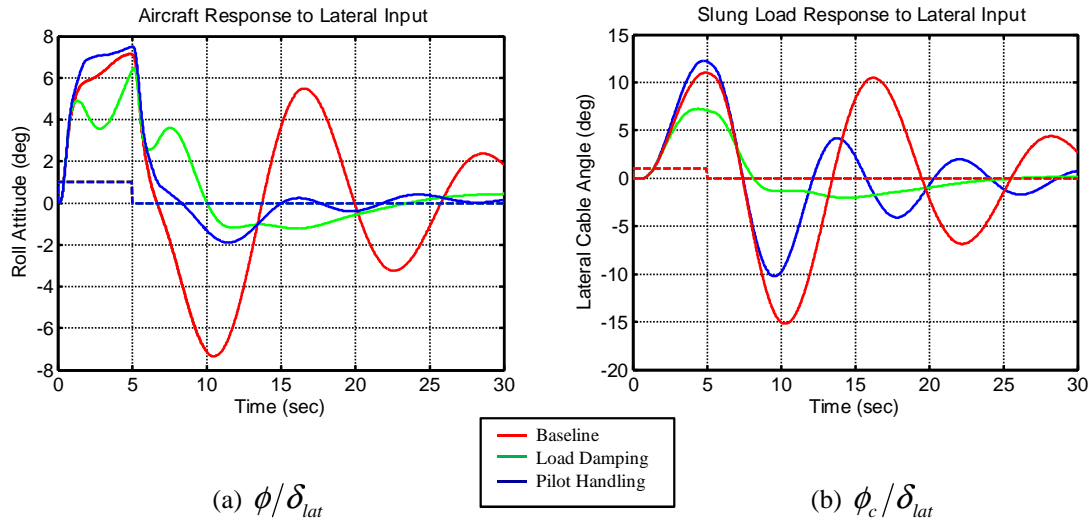


Figure 18: Closed loop time response overlays for three optimized control systems.

VII. Nonlinear Pilot in the Loop Simulation

Evaluation in a nonlinear environment was pursued with two objectives: to determine if benefits developed in the linear environment would transfer to a nonlinear full envelope flight simulation, and to perform realistic piloted simulation. The GenHel nonlinear model of the UH-60 and external load, discussed in Sec. II, was used for the nonlinear dynamics simulation. To provide a visual environment, the RIPTIDE[®] software is used to realize real time, visual, full-flight-envelope pilot in the loop simulation.²⁸ RIPTIDE[®] provides the integration between the SIMULINK control system, GenHel, visual environment, and pilot interceptors.

A. Nonlinear Environment Considerations

In the nonlinear environment, which uses full large angle equations, careful consideration of the load feedbacks must be taken into account. In a field application airworthy direct measurements of cable angle and rate would be desirable, but are only just now under development. Therefore, in this research, the load Euler angles and angular rates will be measured in an EGI unit on board the load. This means that load angles and rates will be measured with respect to the load body axes. Considering that the load can spin with respect to the helicopter and the helicopter can yaw with respect to the load, it is important to transform the load Euler angles and rates into a coordinate system that is aligned with the aircraft heading, which we call the ‘‘cable angle’’. This ensures that the lateral and longitudinal load motion with respect to the helicopter will be feedback to the appropriate control axis, with the proper sign.

For the transformation of load Euler angles to cable Euler angles, we assume that the load does not pitch or roll about the cable. This is a very good assumption for the flight condition and type of external load that is considered here; a rectangular load at low speed conditions. From this assumption, the direction vector along the cable is equivalent in either the load or cable coordinate system. Then, resolving the cable direction (\hat{c}_z and \hat{l}_z) into inertial coordinates using both the load Euler angles and the aircraft-aligned heading cable-angle transformation gives:

$${}^N R^H * {}^H R^C * \begin{bmatrix} 0 \\ 0 \\ 1 \end{bmatrix}_{\hat{c}_x, \hat{c}_y, \hat{c}_z} = {}^N R^L * \begin{bmatrix} 0 \\ 0 \\ 1 \end{bmatrix}_{\hat{l}_x, \hat{l}_y, \hat{l}_z} \quad (13)$$

The key coordinate systems are shown in Fig. 19, and described in Table 6.

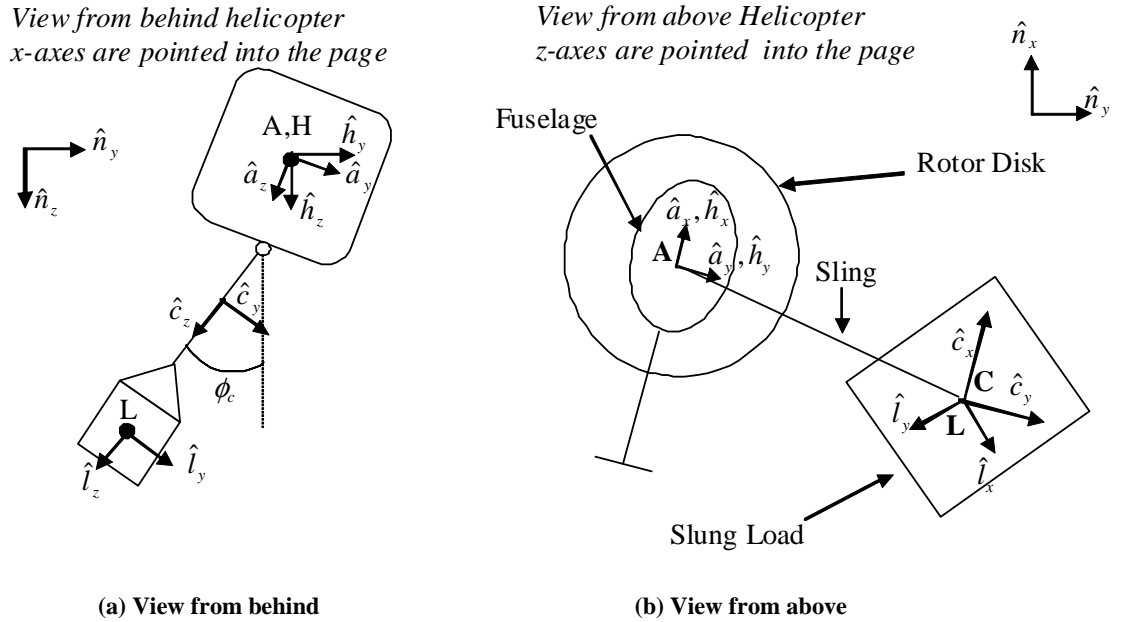


Figure 19. Coordinate systems for cable angle feedback.

Table 6. Definition of reference frames.

Reference Frame	Description	Details
N	Inertial Frame	Standard inertial frame
H	Aircraft Level Heading Frame	Aligned with aircraft heading, but does not pitch or roll
A	Aircraft Body Axis Frame	Yaws, pitches and rolls with the aircraft
C	Cable Frame	Aligned with the cable (does spin relative to the aircraft)
L	Load Body Frame	Yaws, pitches and rolls with the load

${}^N R^H$ represents the rotation/transformation matrix from aircraft level heading (H) coordinate system to the inertial coordinate system (N). The level heading coordinate system is aligned with the aircraft heading, but does not pitch or roll with the fuselage.

$${}^N R^H = \begin{bmatrix} C_\psi & -S_\psi & 0 \\ S_\psi & C_\psi & 0 \\ 0 & 0 & 1 \end{bmatrix} \quad (14)$$

where $S_\psi = \sin\psi$ and $C_\psi = \cos\psi$.

${}^H R^C$ represents the transformation matrix from the cable frame (C) to the level heading coordinate frame (H) and ${}^N R^L$ represents the rotations between the load frame (L) and the inertial coordinate frame (N). The load frame spins with the load body, whereas the cable coordinate system is aligned with the aircraft heading as shown in Fig. 19b.

$${}^H R^C = \begin{bmatrix} C_{\theta_c} & S_{\phi_c} S_{\theta_c} & C_{\phi_c} S_{\theta_c} \\ 0 & C_{\phi_c} & -S_{\phi_c} \\ -S_{\theta_c} & S_{\phi_c} C_{\theta_c} & C_{\phi_c} C_{\theta_c} \end{bmatrix} \quad (15)$$

$${}^N R^L = \begin{bmatrix} C_{\theta_l} C_{\psi_l} & S_{\phi_l} S_{\theta_l} C_{\psi_l} - C_{\phi_l} S_{\psi_l} & C_{\phi_l} S_{\theta_l} C_{\psi_l} + S_{\phi_l} S_{\psi_l} \\ C_{\theta_l} S_{\psi_l} & S_{\phi_l} S_{\theta_l} S_{\psi_l} + C_{\phi_l} C_{\psi_l} & C_{\phi_l} S_{\theta_l} S_{\psi_l} - S_{\phi_l} C_{\psi_l} \\ -S_{\theta_l} & S_{\phi_l} C_{\theta_l} & C_{\phi_l} C_{\theta_l} \end{bmatrix} \quad (16)$$

where ϕ_c and θ_c are the cable Euler angles with respect to the level heading frame. ϕ_l , θ_l , and ψ_l are the load Euler angles with respect to the inertial frame.

In this case, the aircraft heading and the load Euler angles are the measured quantities on the aircraft. Rearranging known quantities to the right half side of Eq. 13 gives:

$${}^H R^C * \begin{bmatrix} 0 \\ 0 \\ 1 \end{bmatrix}_{\hat{c}_x, \hat{c}_y, \hat{c}_z} = {}^H R^N * {}^N R^L * \begin{bmatrix} 0 \\ 0 \\ 1 \end{bmatrix}_{\hat{l}_x, \hat{l}_y, \hat{l}_z} \quad (17)$$

Which is equivalent to:

$$\begin{bmatrix} C_{\phi_c} S_{\theta_c} \\ -S_{\phi_c} \\ C_{\phi_c} C_{\theta_c} \end{bmatrix} = \begin{bmatrix} C_\psi & S_\psi & 0 \\ -S_\psi & C_\psi & 0 \\ 0 & 0 & 1 \end{bmatrix} * \begin{bmatrix} C_{\phi_l} S_{\theta_l} C_{\psi_l} + S_{\phi_l} S_{\psi_l} \\ C_{\phi_l} S_{\theta_l} S_{\psi_l} - S_{\phi_l} C_{\psi_l} \\ C_{\phi_l} C_{\theta_l} \end{bmatrix} \quad (18)$$

Solving for the cable angles gives the required angles for feedback, in terms of the measured load Euler angles and aircraft heading:

$$\phi_c = \arcsin \left(- \begin{bmatrix} -S_\psi & C_\psi & 0 \end{bmatrix}^* \begin{bmatrix} C_{\phi_1} S_{\theta_1} C_{\psi_1} + S_{\phi_1} S_{\psi_1} \\ C_{\phi_1} S_{\theta_1} S_{\psi_1} - S_{\phi_1} C_{\psi_1} \\ C_{\phi_1} C_{\theta_1} \end{bmatrix} \right) \quad (19)$$

$$\theta_c = \arctan \left(\frac{\begin{bmatrix} C_\psi & S_\psi & 0 \end{bmatrix}^* \begin{bmatrix} C_{\phi_1} S_{\theta_1} C_{\psi_1} + S_{\phi_1} S_{\psi_1} \\ C_{\phi_1} S_{\theta_1} S_{\psi_1} - S_{\phi_1} C_{\psi_1} \\ C_{\phi_1} C_{\theta_1} \end{bmatrix}}{\begin{bmatrix} 0 & 0 & 1 \end{bmatrix}^* \begin{bmatrix} C_{\phi_1} S_{\theta_1} C_{\psi_1} + S_{\phi_1} S_{\psi_1} \\ C_{\phi_1} S_{\theta_1} S_{\psi_1} - S_{\phi_1} C_{\psi_1} \\ C_{\phi_1} C_{\theta_1} \end{bmatrix}} \right) \quad (20)$$

It is simple to transform the load referenced angular velocities to the cable axes, with the transformation between load and cable coordinates:

$${}^c R^L = \begin{bmatrix} \cos \Delta\psi & \sin \Delta\psi & 0 \\ -\sin \Delta\psi & \cos \Delta\psi & 0 \\ 0 & 0 & 1 \end{bmatrix} \quad (21)$$

where $\Delta\psi = \psi - \psi_1$

B. Validation of Control System in Nonlinear Environment

To ensure that the nonlinear simulation with the control system engaged would behave as predicted in the linear environment, a validation of the nonlinear system against the linear system was performed in the frequency domain. In order to determine frequency responses from the nonlinear simulation, a frequency sweep is played into the pilot inceptor. The aircraft and load response was measured as a result of the sweep inputs. Then, the data is transformed to the frequency domain via the ChirpZ transform using the CIFER[®] software.²¹ This method ensures that the linear predicted frequency domain handling qualities predictions will hold up in the nonlinear simulation. In order to provide a good validation, the linear model must be an accurate representation of the nonlinear model, and the integration between the nonlinear model and control system must be correctly implemented in the nonlinear environment. The validation was sufficiently accurate in all axes, as demonstrated for the roll attitude and cable angle responses in Figs. 20-21. There is excellent agreement near the load mode (~1 rad/s), which is of key importance to this study. The small discrepancy between 5-8 rad/s is due to an effectively more heavily damped rotor flap regressing mode in the nonlinear simulation. This should not have a large effect on the handling qualities because the differences are small at a frequency where the pilot rarely operates (as indicated by pilot cutoff frequencies calculated in the following section of this paper).

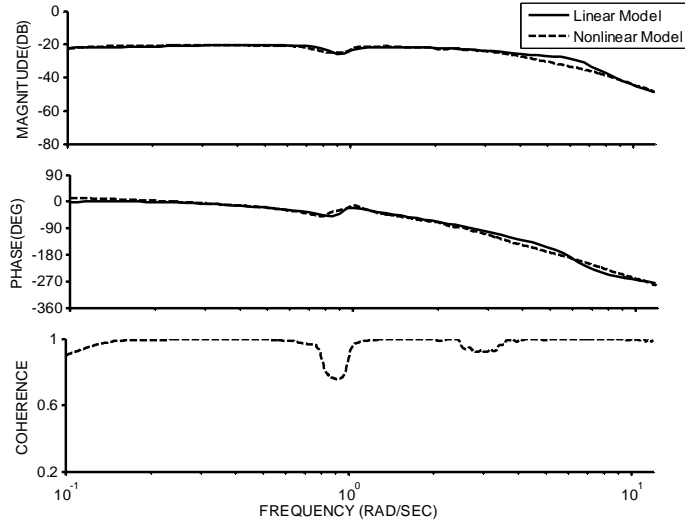


Figure 20. ϕ/δ_{lat} closed loop validation of nonlinear responses for the pilot handling control system.

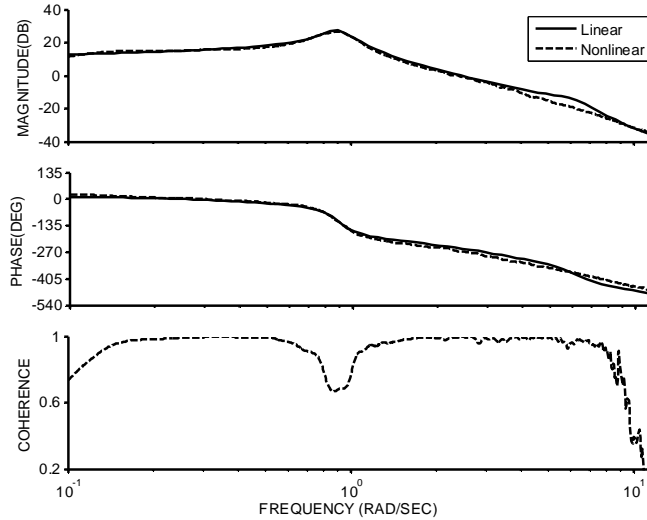


Figure 21. ϕ_c/δ_{lat} closed loop validation of nonlinear responses for the pilot handling control system.

VIII. Pilot Simulation

Given the good agreement between the linear and nonlinear simulation models, the next step was to test the control systems with a pilot in the loop to determine whether the predicted results from the linear analysis were realized. The simulation was performed on AFDD's fixed base Human Factors Simulation Cab at Ames Research Center. This cab uses a side-stick for longitudinal and lateral controls, and conventional pedal and collective. Although the actual RASCAL UH-60 helicopter has a center stick configuration, this simulation still allows us to compare and contrast the relative performance of the control systems.

The simulator display is shown in Fig. 22. There is a standard forward view (window A) and the UH-60 CAAS display panel (window B). The load is displayed to the pilot in a downward view (window C), as though a camera were looking down at the load. This is in fact the view as seen by the "crew chief", who watches the load motion via an open hatch in the back of the UH-60. This display is used here to provide the pilot a load motion cue, since he/she cannot feel the load in the fixed base simulation. The downward view also gives the pilot visual cues for the lateral and longitudinal reposition maneuvers given the limited view out the forward window.

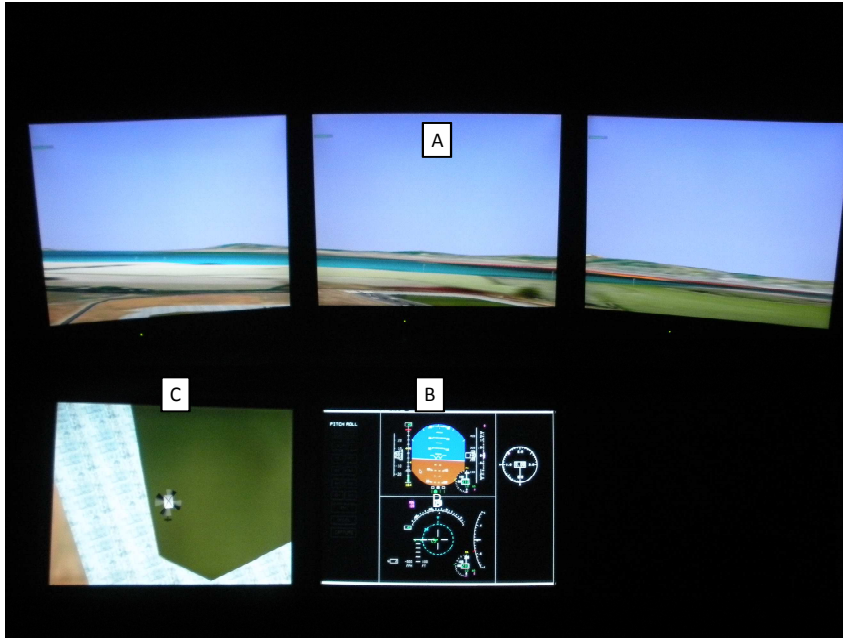


Figure 22. Simulator displays.

Due to the limitations of the fixed base environment for simulating slung load configurations, and the lack of sideward visual cueing (no side window), handling qualities rating would not be valid and were not collected. Instead, pilot comments comparing the two cable angle feedback control systems to the baseline, as well as statistical data (pilot stick cutoff frequency) are used to evaluate the relative drawbacks and benefits of the cable angle feedback control systems. Formal flight test evaluations in the RASCAL will be performed in the upcoming months (see Section VIII, Future Plans), where handling qualities ratings will be collected.

A. Piloted Tasks

The pilots were asked to complete a series of evaluation maneuvers and provide comments for each of the three control systems. The flight condition was hover/low speed, 15000lbs aircraft, 5000lbs load, and 79ft sling. Pilots first flew the baseline control system, and then in random order, the two cable angle feedback control systems for the tasks given in Table 7. Comments were collected after each task in Table 7 for each control system. Pilots were instructed to provide comments comparing and contrasting the control systems and the relative ease of each of the tasks.

Four pilots were used in this study. All four pilots were test pilots, with UH-60 slung load experience. Pilots 1, 3, 4 are US Army experimental test pilots. Pilot 2 is a retired NASA test pilot.

Table 7. Pilot tasks.

Task #	Task	Description
1	Check out/ Familiarization	Pilot should become familiar with the response of the control system before performing the tasks.
2	Lateral Reposition	Fly 6kts laterally across the runway, and return to hover at the far end. This uses the downward display to provide visual references.
3	Longitudinal Reposition	Fly 6kts longitudinally across the runway, and return to hover at the far end. This uses the downward display to provide visual references.
4	Hover Boards	Hover in front of the hover board with and without turbulence.

B. Piloted Comments

The pilot comments provide good insight into the relative merits and drawbacks of the three control systems. A summary of comments are provided for each control system.

1. Baseline FCS

The pilots generally found the baseline control system to have a reasonable response with respect to other external load configurations they have flown and did not find the responses objectionable:

- “Control responses are reasonable” – Pilot 1
- “Dynamics are appropriate to task” – Pilot 2

The lateral reposition task was found to be the most difficult with the external load:

- “Better behaved longitudinally than laterally” – Pilot 2
- “Lateral reposition task is more difficult if not anticipating load motion” – Pilot 3

The pilots also found that the load swing tended to cause a velocity response that was not as smooth and that the load took a long time to damp out:

- “More difficult to maintain speed when starting maneuver while load is still swinging” – Pilot 3
- “Load takes considerable time to damp out, but does not affect workload” – Pilot 1
- “Must accept load oscillations and correct for velocity changes due to load swing” – Pilot 4

2. Damping FCS

The pilots immediately noticed that the load damped more quickly:

- “Load motions damp very quickly as compared to baseline” – Pilot 3
- “Work load roughly same as baseline, but load damps out more quickly” – Pilot 1

The tasks were generally considered easier or the same as baseline, but the pilot must give up some control to the attitude control system:

- “Control is not fine grained, but direction and speed of vehicle easier to control” – Pilot 2
- “Overall maneuver is easier to perform than baseline. [Periodically] got into load oscillations aggravated by the pilot during deceleration and had to back out of the loop” – Pilot 4
- “Longitudinal and lateral repositioning tasks are easier but pilot must give up a lot of control” – Pilot 3

The uncommanded attitudes used to damp the load motions were found to be very unnatural by the 3rd pilot:

- “Unnatural response, can get positive roll angle with negative lateral inputs at times” – Pilot 3
- “Treat the control system like ‘Attitude Suggestion’ as opposed to attitude command” – Pilot 3
- “Must take myself out of the loop and let the aircraft take care of the load” – Pilot 3

3. Pilot Handling FCS

This control system was found to provide a more stable response:

- “More stable velocity response” – Pilot 1
- “Load is more active but a/c is not as driven by the load dynamic, the attitude is more stable even though the load is swinging” – Pilot 2

Pilot #3 found this response to be much more natural than the damping control system:

- “Aircraft is doing the same thing I want to do with the attitude, so more comfortable” – Pilot 3
- “Very natural response” – Pilot 3

All four pilots felt that tasks were easier to complete as compared to the baseline and damping configurations:

- “Good position hold, vehicle response is smooth” – Pilot 1
- “By far the best performance of the three configurations” – Pilot 2
- “This configuration was the easiest to fly, almost as easy as without an external load” – Pilot 3
- “Slightly easier to perform tasks than damping configuration, much better than baseline configuration” – Pilot 4

C. Statistics

The piloted cutoff frequency is an indication of the bandwidth of the pilot's inputs. The pilot cutoff frequency ω_1 is the half power frequency associated with σ_1^{21} in Eq. (19).

$$\sigma_1^2 = \frac{1}{2\pi} \int_0^{\omega_1} G_{\delta\delta}(\omega) d\omega, \quad \left(\frac{\sigma_1}{\sigma_{tot}} \right)^2 = 0.5 \quad (19)$$

The input autospectrum $G_{\delta\delta}$ is calculated via FFT of the input signal within the CIFER[®] software.²¹

For external load operations, it has been observed that the pilot cutoff frequency is typically below the load mode for larger LMRs (including the LMR of 0.25 used here), indicating that the pilot adopts a control strategy to avoid exciting the load motion.² This implies that the pilot cannot fly aggressively with external loads which have long slings and thus low natural frequencies. This may limit the ability to fly some tasks successfully.

The results of the pilot cutoff frequency study indicate that the load damping control system has a much lower pilot cutoff frequency than either the baseline or pilot handling control systems in both the lateral (Fig. 23) and longitudinal axes (Fig. 24). This would indicate a diminished capability to achieve the same aggressiveness as the other two designs, which is consistent with the pilot comments indicating this configuration is not preferred. The pilot handling FCS had a consistently higher piloted cutoff frequency in both axes than the other control systems. In the longitudinal axis, most of the frequencies are much lower than in the lateral axis. However, the cutoff frequencies for the three control systems in the longitudinal axis still follow the same trend as the lateral axis. These results indicate that the pilot handling control system allows the pilots to be more aggressive even in the presence of the load motion. This is consistent with the pilot comments indicating that this was the preferred configuration.

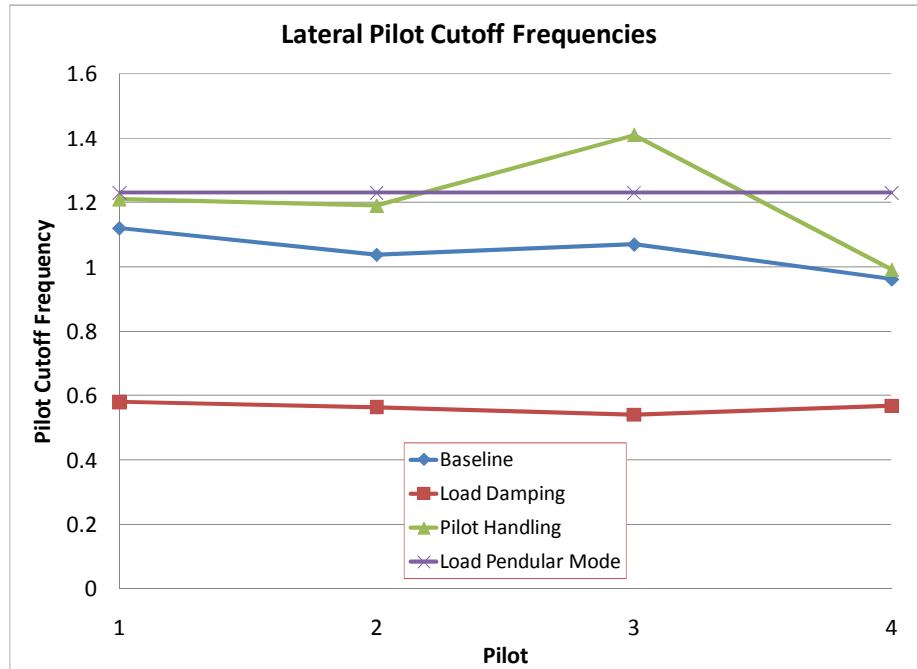


Figure 23. Lateral pilot cutoff frequencies.

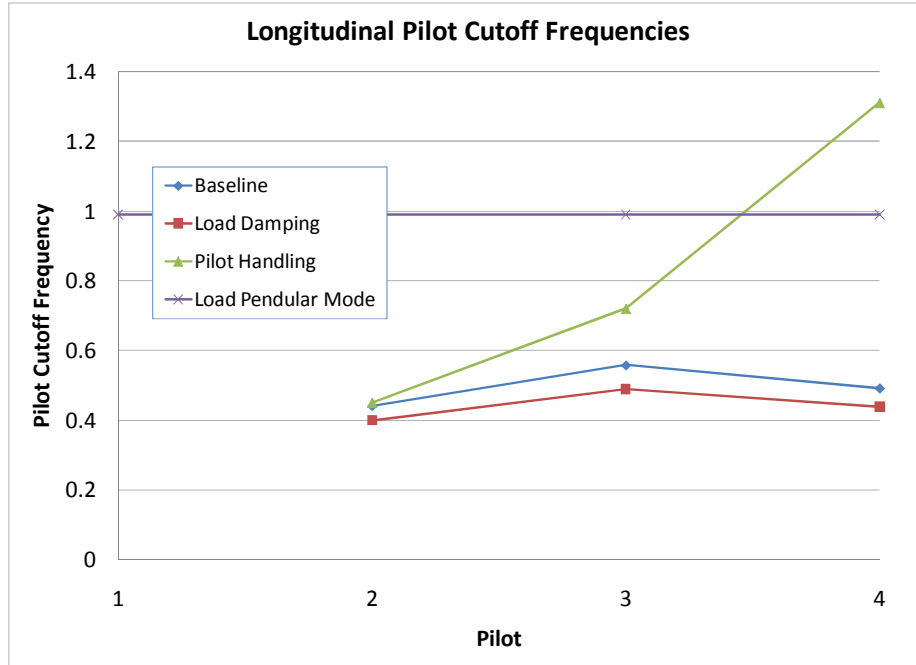


Figure 24. Longitudinal pilot cutoff frequencies (pilot 1 did not perform this task).

IX. Discussion

The results of the analytical and pilot simulation results are consistent with a trade-off between handling qualities and load damping for cable angle feedback control laws. The piloted comments shows a preference for a cable angle feedback configuration that reduces the depth of the notch associated with the aircraft attitude attenuation at the load mode (ΔMAG) over the baseline and load damping configurations. However, for precision load placement, there are clearly operational advantages to being able to quickly damp load motions automatically, despite the cost paid in maneuvering handling qualities. As an example of the benefits of load damping, Fig. 25 shows the lateral reposition maneuver from the fixed based piloted simulation (Pilot #3). In the first 30 seconds of the record, the pilot accelerates to ~10kts, translates across the runway, and decelerates to hover. In the recovery phase, which starts at about 30 seconds for all three cases, the pilot is attempting to hold a stable hover. The load damping case has no load swing nearly immediately after hover is achieved. The other two control laws still have significant load swing when the record ends. The load damping control laws would clearly be useful if the load was being delivered to a precise target location, where for the 79ft sling used herein even a seemingly small five degrees of load swing (in a steady hover) causes 7ft of load translation along the ground.

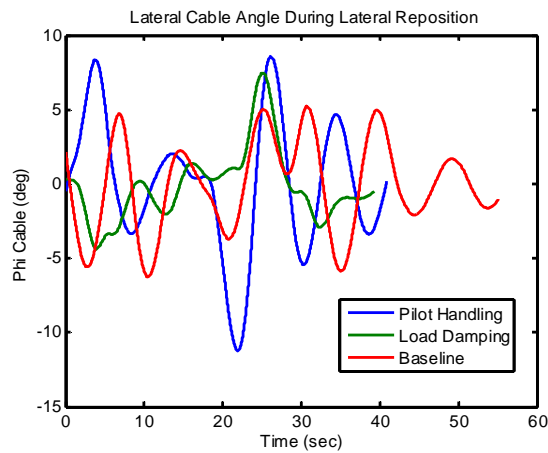


Figure 25. Lateral cable angle during lateral reposition maneuver in fixed based simulator.

There are two solutions to this fundamental tradeoff. The first is to choose a compromise design which is somewhere between the pilot handling and load damping cases, but is not optimal for pilot handling or load damping. The second solution is to switch between the control laws in a task tailored strategy. This could be either a pilot selectable or an automatic load damping switch near hover but would default to the pilot handling control laws during maneuvering. This task tailored method would ensure that the control laws are optimal for the task, but comes at the cost of added complexity due to gain scheduling considerations.

X. Future Plans

The next phase of this research will develop a load positioning control system for precision load placement, which integrates the task tailored method of switching between load damping and pilot handling cable angle feedback control laws. This will enable the pilot to maneuver using the pilot handling control system, then at low speed switch to load damping control laws with the stick in detent. This should improve time and ease of precision load placement as well as improve handling qualities for external load operations.

The final phase of this work will be to test these concepts in flight aboard the UH-60 RASCAL fly-by-wire aircraft. This will determine whether it is feasible and beneficial to measure load motions and use them for feedback parameters in a fly-by-wire control system. The handling qualities will be tested via the ADS-33E-PRF mission task elements and Cooper Harper ratings will be collected.

XI. Conclusions

The importance of carrying external loads with helicopters calls for improved control systems to help minimize pilot workload during these operations. An attitude command explicit model following control system with cable angle feedback was designed using multi-objective optimization to meet hover/low speed handling qualities requirements, disturbance rejection and stability margins. The pilot handling cable angle feedback control system were tested in simulation and determined to be improved over the baseline and load damping control systems. The main conclusions of the paper are:

- 1) The drawbacks of the conventional fuselage feedback control system are degraded handling qualities (HQR <4), and low lateral phase margins near the load mode.
- 2) Cable rate feedback provides damping to the load response. However, load damping is associated with poor aircraft attitude response, and was not preferred by the pilots due to the uncommanded attitudes that result in order to damp the load motions.
- 3) Cable angle feedback combined with fuselage feedback provides improvement in the fuselage response of the aircraft, improving the load handling qualities, and making the aircraft easier to fly.
- 4) Lateral pilot cutoff frequencies higher or equal to the load mode natural frequency can be achieved via cable angle feedback in simulation, which allows the pilot to fly more aggressively and are associated with improved pilot comments.

XII. References

- ¹Franklin, G.F., Powell, J.D., Emami-Naeini, A., Feedback Control of Dynamic Systems 6th Ed., Pearson Prentice Hall, NJ, 2010, pp. 243 -247.
- ²Lusardi, J.A, Blanken, C.L., Braddom, S.R., Cicolani, L.S., Tobias, E.L., "Development of External Load Handling Qualities Criteria," Proceedings of the American Helicopter Society 66th Annual Forum, Phoenix, AZ, May 11-13 2010.
- ³Garnett, T.S., Jr., Smith, J.H., Lane, R., "Design and Flight Test of the Active Arm External Load Stabilization System," Proceedings of the American Helicopter Society 32nd Annual Forum, Washington D.C., May 10-12 1976
- ⁴Gera, J., Farmer, S.W., Jr., "A method of Automatically Stabilizing Helicopter Sling Loads," NASA Technical Note D-7593, July 1974.
- ⁵Dukes, T.A., "Maneuvering Heavy Sling Loads Near Hover Part I: Damping the Pendulous Mode," Proceedings of the American Helicopter Society 28th Annual Forum, May 1972.
- ⁶Gupta, N.K., Bryson, A.E., Jr., "Automatic Control of a Helicopter with a Hanging Load," NASA Contractor Report 136504, June 1973.
- ⁷Liu, D.T., "In-Flight Stabilization of Externally Slung Helicopter Loads," USAAMRDL Technical Report 73-5, May 1973.
- ⁸Hutto, A.J., "Flight-Test Report on the Heavy-Lift Helicopter Flight-Control System," Proceedings of the 31st Annual Forum of the American Helicopter Society, New York, NY, May 1975.

- ⁹Davis, J., Garnett T., Gaul, J., “Heavy Lift Helicopter Flight Control System – Volume III, Automatic Flight Control System Development and Feasibility Demonstration,” USAAMRDL Technical Report 77-40C, September 1977.
- ¹⁰McGonagle, J.G., “The Design, Test, and Development Challenges of Converting the K-MAX Helicopter to a Heavy Lift Rotary Wing UAV,” Proceedings of American Helicopter Society 31st Annual Forum, Washington, D.C., May 9-11 2001.
- ¹¹Bisgaard, M., la Cour Harbo, A., Bendtsen J.D., “Input Shaping for Helicopter Slung Load Swing Reduction,” AIAA Guidance Navigation and Control Conference, Honolulu, HI, August 2008.
- ¹²Bisgaard, M., la Cour Harbo, A., Bendtsen J.D., “Swing Damping for Helicopter Slung Load Systems Using Delayed Feedback,” AIAA Guidance, Navigation, and Control Conference, Chicago, Illinois, August 2009.
- ¹³Anon., Aeronautical design Standard, Handling Quality Requirements for Military Rotorcraft, ADS-33E-PRF, U.S. Army Aviation and Missile Command (USAAMCOM), 2000.
- ¹⁴Sahasrabudhe, V., et al., “Balancing CH-53K Handling Qualities and Stability Margin Requirements in the Presence of Heavy External Loads”, Proceedings of the 63rd American Helicopter Society Annual Forum, Virginia Beach, VA, May 1-3, 2007.
- ¹⁵Hamers, M., von Hinuber, E., Richter A., “CH53G Experiences with a Flight Director for Slung Load Handling”, Proceedings of the 64th American Helicopter Society Annual Forum, Montreal Canada, April 29- May 1st, 2008.
- ¹⁶Brenner, H., “Helicopter Sling Load Positioning,” Proceedings of the 35th Annual European Rotorcraft Forum, Germany, Sept. 2009.
- ¹⁷Brenner,H., “Helicopter Sling Load Pendulum Damping,” Proceedings of the 35th Annual European Rotorcraft Forum, Germany, Sept. 2009.
- ¹⁸Morales III, E., Hindson, W.S., Frost, C.R., Tucker, G.E., Arterburn, D.R., Kalinowski, K.F., Dones, F., “Flight Research Qualification of the Army/NASA RASCAL Variable Stability Helicopter,” Proceedings of the American Helicopter Society 58th Annual Forum, Montreal, Canada, June 2002.
- ¹⁹Howlett, J.J., “UH-60 Black Hawk Engineering Simulation Program: Volume 1 – Mathematical Model,” NASA Technical Report CR-166309, 1981
- ²⁰Tyson, P.H., “Simulation Validation and Flight Prediction of UH-60A Black Load Helicopter/Slung Load Characteristics,” Naval Post Graduate School Master’s Thesis, Monterey, CA, March 1999.
- ²¹Tischler, M.B., Remple, R.K., Aircraft and Rotorcraft System Identification, AIAA, Reston, VA, 2006.
- ²²Hoh, R.H., Mitchell D.G., Aponso, B.B., Key, D.L, Blanken, C.L., “Background Information and User’s Guide for Handling Qualities Requirements for Military Rotorcraft,” USAAVSCOM Technical Report 89-A-008, Dec 1989.
- ²³McRuer, D., Ashkenas, I., Graham, D., Aircraft Dynamics and Automatic Control, Princeton University Press, Princeton, NJ, 1973.
- ²⁴Tischler, M.B, Ivler, C.M., Mansur, M.H., Cheung, K.K., Berger, T., Berrios, M., “Handling-Qualities Optimization and Trade-offs in Rotorcraft Flight Control Design,” Proceedings of the RAeS Rotorcraft Handling-Qualities Conference, University of Liverpool, U.K., 4-6 Nov 2008.
- ²⁵Horowitz, I., M., Synthesis of Feedback Systems, Academic Press.
- ²⁶Fujizawa, B.T., “Control Law Design and Validation for a Helicopter In-Flight Simulator”, California Polytechnic State University Master’s Thesis, San Luis Obispo, CA, February, 2010.
- ²⁷Tischler, M. B., Colbourne, J. D., Morel, M. R, Biezd, D. G., Cheung, K. K., Levine, W. S., and Moldoveanu, V., “A Multidisciplinary Flight Control Development Environment and Its Application to a Helicopter,” IEEE Control System Magazine, Vol. 19, No. 4, August 1999, pp. 22-33.
- ²⁸Mansur, M.H., Dai, W., RIPTIDE Installation and User’s Guide, University Affiliated Research Center.